JOURNAL OF Materials CHEMISTRY

Formation of hydrogenated Si_2O films by UV laser photolysis of disiloxane

Josef Pola,*[a] Markéta Urbanová,[a] Zdeněk Bastl,[b] Jan Šubrt[c] and Helmut Beckers[d]

[a]*Academy of Sciences of the Czech Republic, Institute of Chemical Process Fundamentals, 165 02 Prague 6, Czech Republic*
[b]*The J. Heyrovský Institute of Physical Chemistry, 182 23 Prague 8, Czech Republic*
[c]*Institute of Inorganic Chemistry, 25 068 Řež near Prague, Czech Republic*
[d]*Anorganische Chemie, FB 9, Universitat-GH, W-5600 Wuppertal 1, Germany*

Received 19th May 1999, Accepted 7th July 1999

ArF laser-induced photolysis of disiloxane in the gas phase results in the cleavage of the Si–H bonds and affords chemical vapour deposition of novel hydrogenated silicon suboxide films. The films are sensitive to ambient atmosphere and were characterised by FTIR and XP spectroscopy and by SEM.

Introduction

Hydrogenated amorphous silicon-rich Si_xO_y films have had a diverse range of applications in recent decades. There has also been interest in chemical vapour deposition (CVD) of amorphous suboxides of silicon, a-SiO_x : H (*e.g.* refs. 1 and 2) and in the Si_2O molecule which, although investigated theoretically[3,4] and considered as an entity in interstitial oxygen in silicon[5,6] has not yet been unequivocally characterized.[7] In conjunction with our previous studies on laser-induced CVD of Si/O and Si/C/O materials (*e.g.* refs. 8–10) we have examined IR laser thermolytic decomposition of disiloxane, $H_3SiOSiH_3$ (DSO), and revealed[11] that this reaction is dominated by elimination and polymerization of transient silanone $H_2Si{=}O$ and that it represents a convenient process for the preparation of poly(hydridosiloxane) $-(H_2SiO)_n-$ films.

Here, we report on UV laser photolysis of DSO and show that this process is remarkably different from the IR laser induced decomposition, since it is controlled by the scission of the Si–H and not Si–O bonds, and allows production of solid materials the composition of which corresponds to hydrogenated Si_2O polymers.

Experimental

Experiments were performed using an ArF (ELI 94 model) laser operating at 193 nm with a repetition frequency of 10 Hz and energy fluence of 200 mJ cm^{-2}. ArF laser irradiation of DSO (0.7 kPa) was carried out in a Pyrex reactor which consisted of two orthogonally positioned tubes (both 2 cm in diameter), one (10 cm long) fitted with NaCl windows and the other (6 cm long) fitted with quartz plates. The reactor was equipped with a Teflon valve which allowed withdrawal of gaseous samples for GC and GC–MS analysis and attachment of the reactor to a vacuum line. The unfocused beam was spatially filtered by an aperture to a size of 1 cm^2 and it entered the reactor through the quartz window.

The progress of the DSO photolysis was monitored by periodically removing the reactor and placing it in the cell compartment of the FTIR (Nicolet Impact) spectrometer. The pressure of the decomposed DSO was determined from its absorption band at 2169 cm^{-1}. The gaseous samples obtained upon DSO irradiation were also analysed on a Shimadzu model QP 1000 quadrupole mass spectrometer and on a Shimadzu 14A chromatograph coupled with a Chromatopac C-R5A computing integrator. These analyses were performed using Porapak or SE-30 columns, helium or nitrogen as carrier gas, and programmed (20–150 °C) temperature variation. Hydrogen was identified on a Hewlett Packard 5010A gas chromatograph (TCD, carbosieve column).

In order to evaluate the properties of the deposit by FTIR and XP spectroscopy, as well as by scanning electron microscopy, the deposits were produced on different substrates (Cu, KBr) housed in the reactors before the irradiation. The photoelectron spectra were recorded in a VG ESCA 3 Mk II electron spectrometer. The XPS measurements were performed using an Al Kα $h\nu$ (= 1486.6 eV) non-monochromatized source at a power of 220 W. The spherical sector analyzer was operated in the fixed analyzer transmission mode using a pass energy of 20 eV. The background pressure during the spectral accumulation was in the region of 10^{-6} Pa. Quantification of the concentrations of elements was accomplished by correcting the photoelectron peak areas for their cross-sections[12] and accounting for the dependence of analyzer transmission[13] and electron inelastic mean free paths[14] on the kinetic energy of photoelectrons. The accuracy of the measured binding energies was ± 0.2 eV. Scanning electron microscopy studies of the deposits were performed on an ultrahigh-vacuum instrument (Tesla BS 350).

DSO was prepared by reaction of iodosilane with silver oxide in a vacuum manifold and separated from iodosilane by low-temperature distillation. Its purity was checked by IR spectrometry.

Results and discussion

Absorption in the UV region of DSO is known to have maxima at *ca.* 130, 139 and 150 nm and a tail to higher wavelengths,[15] the absorptivity of a gaseous sample at 193 nm (irradiation wavelength of the ArF laser) being 5.9×10^{-4} $Torr^{-1}$ cm^{-1}. Irradiation of DSO (0.7 kPa) with photons at 193 nm resulted in the depletion of DSO and formation of H_2 along with a white solid film which was deposited onto the reactor surface. This film is opaque to 193 nm radiation and detrimental to photolytic progress: *ca.* 10% decomposition of DSO can be achieved within 15 min by irradiation at the one quartz plate, while *ca.* 40% decomposition of DSO is observed after 30 min by irradiation at one (15 min) and then the other quartz plate of the reactor. The fact that hydrogen is observed as the only gaseous product indicates that DSO undergoes cleavage of the Si–H bonds.

Photolytic steps

This reaction can, in principle, take place by a radical mechanism involving homolysis of the Si–H bond [Scheme 1, eqn. (1)], chain reactions [Scheme 1, eqns. (2), (3) and (2′), (3′)] and radical recombinations [Scheme 1, eqns. (4), (4′)]. Starting

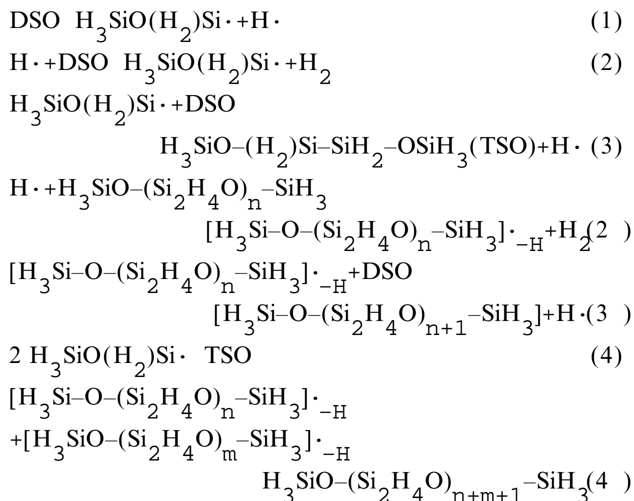

Scheme 1

from trisiloxane (TSO), either linear (A) or branched-chain (B) products can be formed. However, the same final products can be also obtained *via* the sequence of 1,1-H_2 elimination [Scheme 2, eqn. (5)] and silylene insertion [Scheme 2,

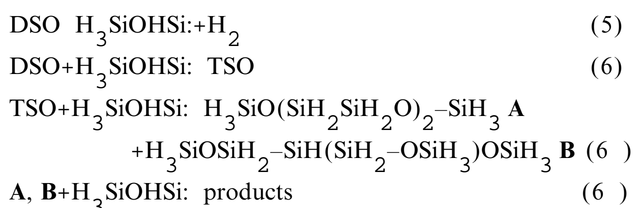

Scheme 2

eqns. (6), (6′), (6″)]. These reactions are well known for monoorganylsilanes $RSiH_3$ (*e.g.* ref. 16). Differentiation between these mechanisms can be made only by identification of intermediate H atoms and silyloxysilylenes.

A discussion on IR laser-induced decomposition of DSO is relevant, since this process has a totally different reaction course[11] yielding solid material with an O/Si ratio close to 1, and silane (0.75–0.90 mol per mol of DSO decomposed) together with minute amounts of cyclotrisiloxane, cyclotetrasiloxane, trisiloxane and tetrasiloxane. These products and the Arrhenius parameters of this decomposition (log $A = 13.1 \pm 0.8\ s^{-1}$ and $E_a = 234 \pm 8\ kJ\ mol^{-1}$) can only be rationalized in terms of a four-centre cyclic transition state (Scheme 3) during unimolecular decomposition of DSO yielding transient silanone ($H_2Si{=}O$) which mostly polymerizes into $(H_2SiO)_n$, inserts into DSO, and undergoes cyclotrimerization and cyclotetramerization.

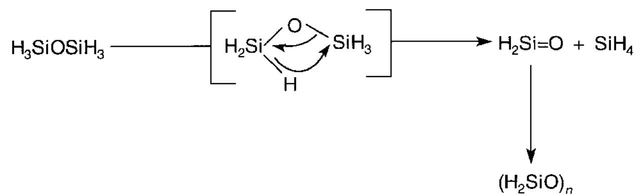

Scheme 3

Composition of the deposited films

The deposited films show IR absorptions (Fig. 1) typical for poly(hydridosiloxanes) $H_xSi_yO_z$. The IR absorption spectra of the UV laser-deposited films consist of bands at ν/cm^{-1} (relative absorptivity): 730 (0.27), 859 (0.71), 972 (0.59), 1079 (1.0), 2186 (0.44) and 2231 (0.19) and can be interpreted[1,17,18] as dominated by a very strong and broad band due to ν(Si–O–Si) and several other bands assignable to $H_nSi(O)$ moieties. It is known that the oxygen and H_nSi bending modes below 1000 cm^{-1} in amorphous SiO_x : H films ($x < 2$) and oxygenated polysilanes,[19–22] are less informative[23] than the Si–H stretching mode in polysilanes which is empirically related to the electronegativity/inductive effect of the neighbouring atoms.[1,18] It is also known that the Si–H stretching mode in fully oxidized $(SiH_2)_x$ polysilanes exhibits[17] bands at 2190 and 2245 cm^{-1}. Hence, the bands at 2183 and 2250 cm^{-1} observed in the deposited films from DSO can be unequivocally assigned to the $H_2Si(O)$ structural unit. Furthermore, the lack of bands at *ca.* 2100 and 2000 cm^{-1} indicates the absence of $(SiH_2)_n$ and $(SiH)_n$ structures[17,24] in which the Si–H bond is isolated from oxygen by at least two silicon atoms. The absorbance ratio $A_{\nu(Si-H)}/A_{\nu(Si-O-Si)}$ in the UV laser-deposited films (0.44) is higher that that in the –$(H_2SiO)_n$– solids obtained by IR laser irradiation (0.26);[11] the former are therefore richer in hydrogen and can be assumed to possess a structure close to –$(H_2Si{-}O{-}SiH_2)_n$–.

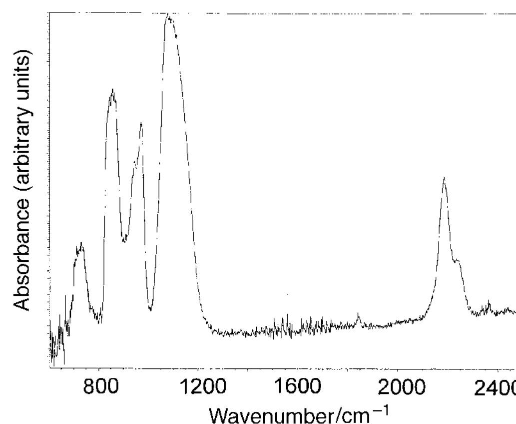

Fig. 1 FTIR spectrum of a film deposited from DSO upon UV laser irradiation.

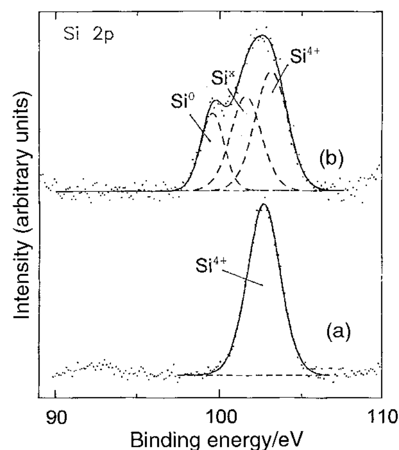

Fig. 2 Photoelectron spectrum of Si 2p electrons ($E = 4.5$ keV, $I = 35$ μA, $t = 3$ min). (a) Native sample and (b) sample sputtered by Ar ions.

The photoelectron spectra of the Si 2p electrons (Fig. 2) in the UV laser-deposited films reveal the presence of only Si^{4+} in the native films and of Si^0, Si^{4+} and Si^x ($0<x<4$) in the films after Ar ion sputtering. Owing to the quasi-amorphous structure of the deposits, the suboxide Si^x ($0<x<4$) component cannot be deconvoluted into contributions of the individual oxidation states of Si. The overall stoichiometry of the films characterized by an O/Si atomic ratio of 1.5–2.5 for the native and 0.8–1.6 for the sputtered films, as well as the population of the assigned chemical states of Si calculated from the peak intensities, $Si^{4+}\approx 1$ in the native and $Si^0:Si^{4+}:Si^x\approx 0.21:0.45:0.34$ in the sputtered films, are in accord with oxidation of the deposits upon exposure to air. The data thus show that the deposits initially possessed more Si than O and that the initially produced hydrogenated silicon suboxide films underwent superficial oxidation when transferred from the reactor to the XP spectrometer.

Scanning electron microscopic (Fig. 3) analysis reveals that the deposited films consist of sub-micrometer sized agglomerates which form a woven texture. This morphological feature indicates that the films are not compact and can be penetrated by gas to a significant depth. This is in agreement with the readiness of their oxidation in air. We anticipate that the films can be modified into more compact structures upon annealing in vacuum or inert gas and that this process may reduce their tendency towards oxidation.

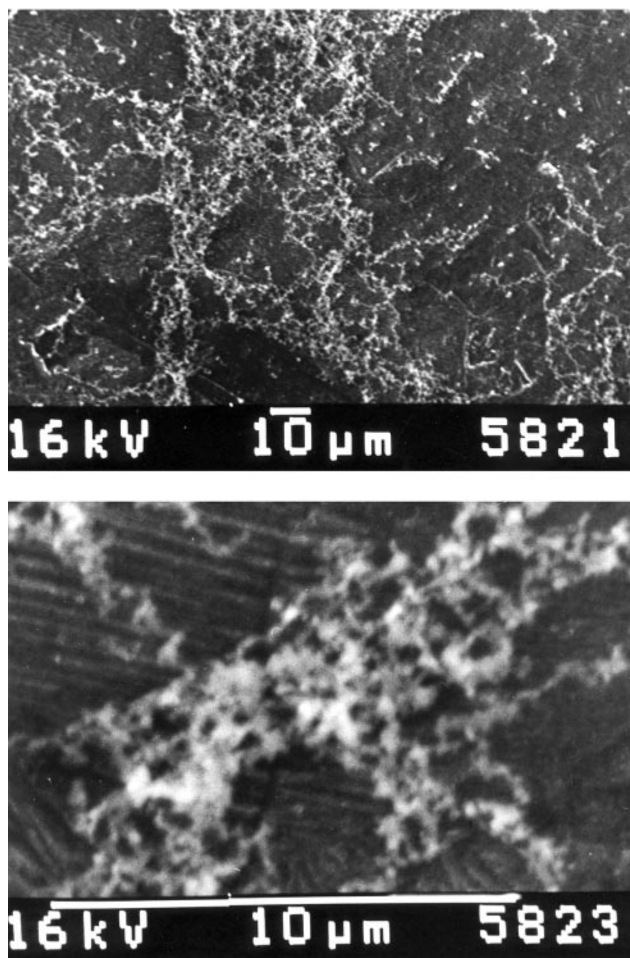

Fig. 3 SEM image of a film deposited from DSO upon UV laser irradiation.

In conclusion, photolysis of gaseous DSO with 193 nm photons results in the cleavage of Si–H bonds and formation of solid hydrogenated silicon suboxide films which can be subsequently oxidized. The results indicate that DSO is a suitable precursor not only for a-Si_2O:H films, but also for Si_2O phases provided that the Si_2O:H films can be dehydrogenated upon annealing. Our results on UV laser-induced decomposition of DSO, along with those on IR laser-induced decomposition of DSO published elsewhere,[11] also reveal that the major decomposition pathway of DSO depends on the laser radiation and occurs *via* dehydrogenation and silane elimination, respectively.

Acknowledgements

The authors thank the Grant agency of the Academy of Sciences of the Czech Republic (grant no. A4072806), the Deutsche Forschungsgemeinschaft and the Fonds der Chemischen Industrie for support.

References

1 D. V. Tsu, G. Lucovsky and B. N. Davidson, *Phys. Rev. B*, 1989, **40**, 1795.
2 M. J. Godbole, D. H. Lowndes and A. J. Pedraza, *Appl. Phys. Lett.*, 1993, **63**, 3449.
3 A. I. Boldyrev, J. Simons, V. G. Zakrzewski and W. von Niessen, *J. Phys. Chem.*, 1994, **98**, 1427.
4 R. L. DeKock, B. F. Yates and H. F. Schaefer III, *Inorg. Chem.*, 1989, **28**, 1680.
5 D. R. Bosomworth, W. Hayes, A. R. L. Spray and G. D. Watkins, *Proc. R. Soc. London, A*, 1970, **317**, 133.
6 B. Pajot, H. J. Stein, B. Cales and C. Naud, *J. Electrochem. Soc.*, 1985, **132**, 3034.
7 R. J. Van Zee, R. F. Ferrante and W. Weltner, *Chem. Phys. Lett.*, 1987, **139**, 426.
8 J. Pola, D. Pokorná, Z. Bastl and J. Šubrt, *J. Anal. Appl. Pyrolysis*, 1996, **38**, 153.
9 J. Pola and H. Morita, *Tetrahedron Lett.*, 1997, **38**, 7809.
10 M. Urbanová, H. Morita, V. Dřínek, Z. Bastl, J. Šubrt and J. Pola, *J. Anal. Appl. Pyrolysis*, 1998, **44**, 219.
11 J. Pola, M. Urbanová, V. Dřínek, J. Šubrt and H. Beckers, *Appl. Organomet. Chem.*, in press.
12 I. M. Band, Yu. I. Kharitonov and M. B. Trzhaskovskaya, *At. Data Nucl. Data Tables*, 1979, **23**, 443.
13 M. P. Seah, in *Practical Surface Analysis*, ed. D. Briggs and M. P. Seah, Wiley, Chichester, 1990, vol. I, p. 201.
14 P. Seah and W. A. Dench, *Surf. Interface Anal.*, 1979, **1**, 1.
15 S. Bell and A. D. Walsh, *Trans. Faraday Soc.*, 1966, **62**, 3005.
16 M. A. Ring, H. E. O'Neal, S. F. Rickborn and B. A. Sawrey, *Organometallics*, 1983, **2**, 1891.
17 P. John, I. M. Odeh, M. J. K. Thomas, M. J. Tricker and J. I. B. Wilson, *Phys. Status Solidi B*, 1981, **105**, 499.
18 G. Lucovsky, J. Yang, S. S. Chao, J. E. Tyler and W. Czubatyj, *Phys. Rev. B*, 1983, **28**, 3225.
19 F. L. Galeener and G. Lucovsky, *Phys. Rev. Lett.*, 1976, **37**, 1414.
20 G. Lucovsky, C. K. Wong and W. B. Pollard, *J. Non-Cryst. Solids*, 1983, **59/60**, 839.
21 G. Lucovsky, R. J. Nemanich and J. C. Knights, *Phys. Rev. B*, 1978, **18**, 4288.
22 W. B. Pollard and G. Lucovsky, *Phys. Rev. B*, 1982, **26**, 3172.
23 *Infrared Structural Correlation Tables and Data Cards*, Heyden & Son Ltd, Spectrum House, London, 1969.
24 H. Shanks, C. J. Fang, L. Ley, M. Cardona, F. J. Demond and S. Kalitzer, *Phys. Status Solidi B*, 1980, **100**, 43.

Paper 9/03998H